Geomechanics and Engineering, *Vol. 40, No. 4 (2025) 239-249*
https://doi.org/10.12989/gae.2025.40.4.239

Settlement control during shield tunneling through soft strata utilizing pre-reinforcement

Yijie Jin[1], Ping Yang*[1], Zhiyu Zhang[2], Lin Li[1], Jiahui Wang[1], Yong Tao[1] and Yanzi Wang[1]

[1]*Department of Civil Engineering, Nanjing Forestry University, Nanjing, China*
[2]*CCCC Tunnel Engineering Company Limited, Nanjing, China*

(*Received October 15, 2023, Revised January 22, 2025, Accepted January 31, 2025*)

Abstract. The rapid expansion of underground transportation systems has given rise to a corresponding increase in the possibility of encountering soft strata, which usually causes substantial ground settlement during shield tunneling. Cement treatment is typically utilized to alleviate ground settlement induced by excavation. However, the implementation of an appropriate reinforcement approach and associated system parameters can be challenging due to the complexity of on-site geological conditions. For long-distance reinforcement projects, this study employs numerical simulations to evaluate the effectiveness of various reinforcement methods and associated system parameters on ground settlement reduction. The simulation results indicate that the triaxial mixing pile (TMP) outperforms the umbrella arch (UA) in settlement reduction and applicability, making it the preferred option for long-distance pre-reinforcement projects. Compared to the scenario without reinforcement, the ground settlement reduction using the UA is limited to 43.7%, while the TMP achieves a reduction of 67.5% with optimal parameters. (i.e. 0.5D (tunnel diameter) reinforcement width, 0.5D depth, 0.5 pile length ratio, 3.0D tunnel buried depth, $1P_{ref} \sim 2P_{ref}$ face pressure, and 22% cement incorporation ratios). These optimal TMP system parameters are also validated through on-site monitoring. Additionally, a new model in which a disturbance correction coefficient $\xi(x)$ is introduced is proposed to predict ground settlement of reinforced strata. The findings presented in this study offer a detailed reference for similar tunnelling projects where ground settlement is a non-negligible concern.

Keywords: numerical simulation; prediction model; pre-reinforcement; settlement reduction; shield tunneling

1. Introduction

Shield tunneling is frequently employed in construction of urban underground tunnels owing to its superiorities in terms of efficiency and safety (An *et al*. 2022). Providing real-time feedback from the impact of continuous shield machine operation on the surrounding conditions can be challenging. To address this issue, ground settlement is typically adopted to characterize this impact during construction. In the past, numerous studies have been dedicated to settlement analysis utilizing different models, including empirical formula model (Peck 1969, O'Reilly and New 1982, Rankin 1988) as well as equivalent stratum loss model (Sagaseta 1987, Liang *et al*. 2015, Deng *et al*. 2022). Peck (1969) proposed the concept of settlement trough curve that follows a Gaussian distribution and developed an empirical model for predicting ground settlement. Subsequently, some researchers modified the Peck model to accommodate different on-site geological conditions (Zhang *et al*. 2022, Song *et al.* 2019). With the introduction of the concept of equivalent stratum loss, the stochastic medium theory, which was initially utilized to predict surface movement and deformation due to coal mining, has been further extended to predict ground settlement in tunnel construction (Verruijt and Booke 1996, Zhou *et al*. 2021). With consideration of the non-uniform distribution of ground loss and shield shell friction, Deng *et al*. (2022) developed a ground loss model for shield tunneling in curved sections. Besides, numerical simulation is frequently utilized to evaluate the soil response to excavation when passing existing structures, as it permits the quantification of ground settlement at different stages of tunneling and can be used to simulate a variety of on-site conditions (Zheng *et al*. 2020, Zhe *et al*. 2018, Qian *et al*. 2019, Zhao *et al*. 2019). This numerical simulation also provides a simplified modeling process for multivariate analysis under complex conditions (Kasper and Meschke 2006, Chakeri *et al*. 2011, Mu *et al*. 2021). As a result, numerical simulation is often adopted for construction plan optimization due to its accuracy, efficiency, and cost-effectiveness.

Underground tunnelling in soft stratum is usually associated with significant ground deformation (Moon *et al*. 2023, Liang *et al*. 2020, Qi *et al*. 2022). To mitigate this issue, cement treatment has been widely used to improve engineering behavior of soft soil by increasing the bearing capacity and enhancing stability in construction (Lv *et al*. 2023, Zhao *et al*. 2021). Several cement treatment techniques (e.g., backfill grouting, rotary jet grouting, mixing pile, and umbrella arch (UA)) are commonly applied on soft soils (Shao *et al*. 2022, Lv *et al*. 2020, Morovatdar *et al*. 2020, Zhao *et al*. 2023). Wherein the pre-reinforcement technique (i.e., rotary jet grouting, mixing

*Corresponding author, Professor
E-mail: yangping@njfu.edu.cn

ISSN: 2005-307X (Print), 2092-6219 (Online)

Table 1 Soil physical and mechanical parameter

Parameter	h* (m)	γ (kN·m^{-3})	E_{ta}(MPa)	E_{se}(MPa)	E_{un} (MPa)	c (kPa)	θ (°)	G (MPa)
Mixed fill	3.0	18.20	4.04	6.06	32.32	6.0	15.0	80.80
Fine sandy clay	12.0	17.30	3.00	4.50	24.00	5.0	24.0	60.00
Mucky silty clay	27.5	17.10	2.50	3.80	20.00	12.7	8.0	50.00
Medium sandy clay	7.8	18.20	3.32	4.98	36.56	4.5	26.5	66.40

*h = thickness; γ = bulk weight; E_{ta} = tangent modulus; E_{se} = secant modulus; E_{un} = unloading modulus; c = cohesion; θ = internal friction angle; G= shear modulus

pile, and UA) is effective in reducing ground settlement compared with post-reinforcement (i.e., backfill grouting) as it can be used to reduce ground settlement before and during excavation.

However, mixing pile, especially triaxial mixing pile (TMP), has gained popularity for its performance in economy and applicability (Phutthananon *et al*. 2021, Yapage *et al*. 2014, Zhao *et al*. 2023). For instance, Pan *et al*. (2022) evaluated the impact of soil-cement mixing pile construction on adjacent shield tunnels. The on-site monitoring results showed that the ground settlement could be reduced to less than 4.3 mm with the help of soil-cement mixing wall. Previous research on TMP focused on the material properties, including the strength properties, permeability, volumetric stability, and durability of the piles (Voottipruex *et al*. 2011, González *et al*. 2009, Consoli *et al*. 2017, Yao *et al*. 2021). In order to enhance mechanical properties of pile, one possible alternative is to mix additives such as fiber, fly ash, and slag (e.g., Shu *et al*. 2022, Pei *et al*. 2015, Zhang *et al*. 2022). Furthermore, a reasonable layout of mixing piles has been proven to improve better resistance to deformation (Liu *et al*. 2012, Phutthananon *et al*. 2021, Zhao *et al*. 2023). Comparative study of deep cement mixing piles and T-shaped deep cement mixing pile by Yi *et al*. (2016) and Phutthananon *et al*. (2020) showed that the T-shaped deep cement mixing pile exhibited better efficacy and less settlement. Yamashita *et al*. (2013) employed a grid-form deep cement mixing wall layout to deal with liquefied sand, which effectively reduced the settlement of soft cohesive soil below the sand layer. Despite widespread application of mixing pile technology, different arrangements of mixing piles are primarily applied to deformation control in highway embankment, and existing research on pre-reinforcement applied to tunnel construction is very limited. Moreover, the impact of corresponding factors on ground settlement is not yet fully understood.

The study aims at providing a comprehensive analysis of the performance of TMP methods and offering practical guidelines for ground settlement control in tunnel construction. The suitability of TMP and UA techniques in controlling ground settlement during tunneling is evaluated. The optimal system parameters, including reinforcement range, pile length ratio, tunnel buried depth, and face pressure, for TMP are also determined through numerical simulations. Subsequently, the optimal system parameters are applied to the shield section project, and a modified model is developed based on on-site monitoring data to predict the ground settlement.

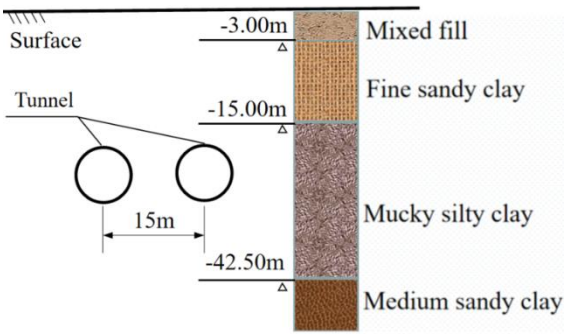

Fig. 1 Overview of the tunnels

2. Project overview

The shield tunnel section from Foshan Line 3 Creative Park Station to Jurong North Road Station is located in the Pearl River Delta of China. The tunnel to be built is composed of double lines, with an outer diameter of 6.2 m. The buried depth of the tunnel ranges from 9.06 m to 21.32 m at a center to center spacing of 15 m. The slurry shield used in the project is 6.45 m in mouth diameter, 6.43 m in tail diameter, 8.2 m in length, and equipped with 0.35 m thick segments made of C50 concrete.

The strata within the depth of the interval survey consists of mixed fill, fine sandy clay, mucky silty clay, and medium sandy clay (Fig. 1). The fundamental properties of the soil strata that the shield passes through have been determined based on a site investigation and laboratory tests as presented in Table 1. Evidently, the tunnel mainly traverses through the mucky silty clay layer which is associated with a low bearing capacity and highly susceptible to disturbance. As a result, the ground surface would suffer from settlement problems and in-place tunnel segments would subject to uplift. Given the complexity and risks posed by the specific site condition, selection of an appropriate reinforcement method is critical for safety during tunnel excavation.

3. Numerical modeling

The section of Foshan Metro Line 3 in China, specifically the DK15+55.764-DK15+112.301 mileage, which crosses through the most unfavorable soil layer, was chosen as the modeling section for the shield tunnel. This section, which spans a length of 57 meters, posed a significant challenge to tunnel construction. To address this issue, pre-reinforcement measures were deemed necessary

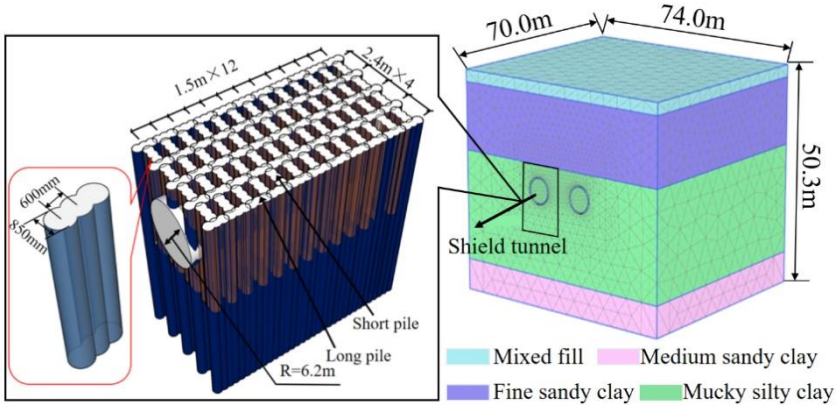

(a) triaxial mixing pile

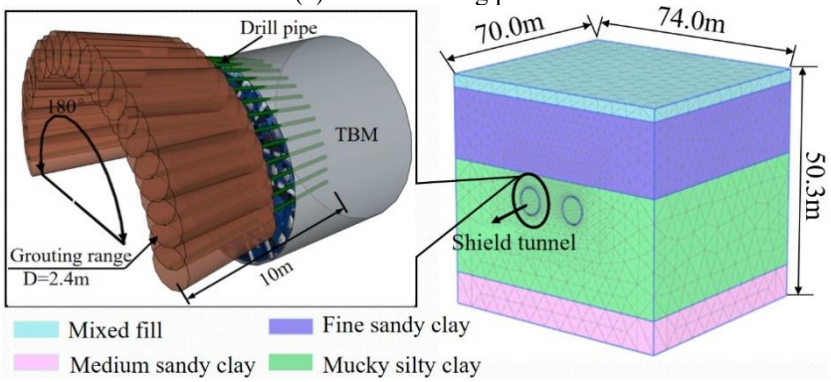

(b) umbrella arch method

Fig. 2 Simulation model for pre-reinforcement

for the soft stratum. This study employed TMP as the pre-reinforcement solution, with UA serving as an alternative option in situations where reinforcement from the ground surface is not optional. In order to investigate the pre-reinforcement technology for reducing ground settlement during shield tunneling in soft strata, numerical simulations and comparative studies on soil deformation were conducted, employing TMP, UA, and no reinforcement. Additionally, several assumptions were made to simplify the modelling and improve the operation efficiency: (1) The soil was homogeneous and linear elastic under undrained condition; (2) All materials were homogeneous, continuous and isotropic, and the soil layer was distributed horizontally in layers; (3) Stratum deformation caused by pre-reinforcement construction was not neglected; (4) Only self-weight of soil and tunnel segment structure was taken into consideration as load and the dynamic load during construction was neglected; (5) The effective range of synchronous grouting behind the wall was set to be the same as the length of the shield tail ring, i.e., 1.5 m; (6) Groundwater seepage was ignored.

3.1 Model establishment

(1) Triaxial mixing pile

A simulation model in which TMPs were applied was developed to achieve better engineering performance and economic efficiency. The model consists of five rows of TMPs at a spacing of 2.4 m along the axial direction of the tunnel. The reinforcement started from 3 m above the tunnel vault to 14.8 m below the arch bottom, with a total height of 24 m. In the direction perpendicular to the axial direction of the tunnel, 13 columns of TMPs were constructed at a spacing of 1.5 m, and the reinforcement started from 3 m above the tunnel vault to 3 m below the arch bottom, with a total height of 12.2 m. Each TMP consists of three circular sections with a diameter of 850 mm and a center-to-center distance of 600 mm as shown in Fig. 2(a).

(2) Umbrella arch method

In the light of previous researches on the optimization of UA technology (Morovatdar *et al*. 2020) and the specific construction requirements of the project, a reinforcement range of 180° along the circumferential direction of the tunnel was chosen for the shield machine arch. To ensure adequate resistance to deformation in the soft stratum, the slurry diffusion radius was set to be 1.2 m and the grouting pipe length was set at 10 m, considering the soil layer distribution at the site and the structural characteristics of the shield machine. The specific layout is shown in Fig. 2(b).

3.2 Model setup

In order to take the influence of size and boundary effect on shield tunneling into consideration, the influence zone of shield construction in all directions was selected to be 3-5 times of the tunnel diameter. Consequently, the dimension of the model was set to be (74×70×50.3) m. To reach high simulation accuracy, the model mesh was set as follows: the

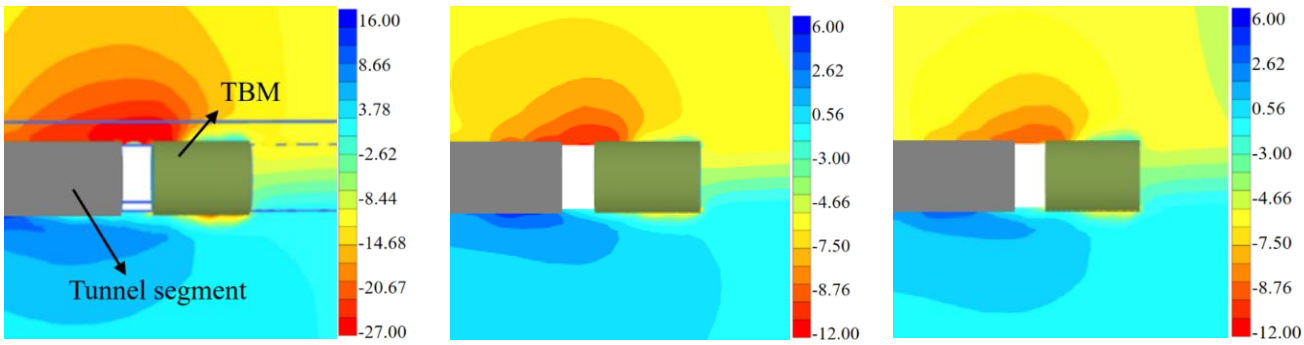

(a) Without reinforcement (b) Umbrella arch method (c) Triaxial mixing pile

Fig. 3 Vertical displacement obtained using distinct reinforcement approaches represents soil settlement,'+' represents soil heave (unit: mm)

Table 2 Physical and mechanical parameters of materials

Parameter	Material model	h (m)	γ (kN·m^{-3})	E_e (MPa)	v*	G (MPa)
Shield machine	Linear elasticity	0.35	120	2.3×10^4	0	11.5×10^3
Cement-soil mixture	Mohr-Coulomb	--	20	165	0.2	60.0
Concrete segment	Linear elasticity	0.35	27	3.1×10^4	0.1	--

*v = Poisson's ratio; E_e = elastic modulus

10-node tetrahedral solid element was adopted to simulate the soil element, reinforced bodies, and tunnel segment with roughness coefficients of 1, 0.5, and 0.3, respectively. The shield machine was simulated using 6-node plate elements, while the contact surface between the shield machine and soil were simulated using 12-node interface elements. Moreover, to simulate the loss of stratum, the face shrinkage of the shield machine was set as (6.45-6.43)/6.43=0.3%. The grouting process was also accounted for, with the grouting pressure set within 1.5 m at the end of the shield to simulate grouting, while the grouting pressure at the upper and lower pipe was set to be 0.2 MPa and 0.25 MPa, respectively. The convergence criterion for numerical analysis is defined by the global error (i.e., force and moment residuals), with a threshold of less than 0.01. This strict standard ensures accurate force equilibrium within the system. Furthermore, each phase was restricted to a maximum of 30 iterations to maintain computational efficiency. This limit prevents excessive computation time while preserving the required accuracy for modeling ground settlement in shield tunneling.

3.3 Mechanical parameters for pre-reinforcement models

A soil constitutive model should be able to capture the stress-strain behavior of soil under diverse loading conditions. Stress redistribution and soil disturbance from shield tunneling in soft ground is usually associated with substantial deformation, characterized by pronounced nonlinear stress-strain behavior. The hardening soil model with small-strain stiffness (HSS) is suitable to simulate soil compressibility through nonlinear constitutive law, which is uniquely superior in simulating soft clay (Benz 2007). Additionally, the HSS model is able to capture plastic flow and shear strength variations in soft soil and is applicable to settlement predictions across various soft soil strata (Schiena *et al*. 2024). Consequently, the HSS model was selected for the simulation in this study. The main material parameters for the HSS were determined through a combination of investigation reports and laboratory studies as presented in Table 2.

3.4 Simulation results

The displacement fields (i.e. axial profile of the tunnel) obtained through different reinforcement approaches are depicted in Fig. 3. The results reveal two similar displacement patterns: (1) During tunneling, the soil layer below the shield experienced a settlement and the soil layer above was subjected to heave due to the compression of soil during shield tunneling. (2) The deformation of the soil occurred mainly at the gap between the shield and the segment due to the release of stress after the excavation. As a result, the soil deformation could be effectively mitigated by timely and synchronous grouting at the shield tail and by appropriately increasing the grouting pressure and volume.

As illustrated in Fig. 3(a), due to the disturbance introduced by tunneling, the maximum settlement of the shield tunnel upon arrival without reinforcement is 26.9 mm, which is not satisfactory for settlement control. The effectiveness of pre-reinforcement in controlling ground settlement is demonstrated in Figs. 3(b) and 3(c) in which the settlement reduced to less than 10 mm after the treatment. Comparing with Fig. 3(a), the deformation of the soil treated by UA or TMP method is significantly lower than that of soil without reinforcement. This is attributed to the hydration of cement which turns the soft soil into a cement-soil mixture with better integrity, water stability, and strength. Consequently, the disturbance to the surrounding soil during tunneling can be significantly reduced with help of the UA or TMP.

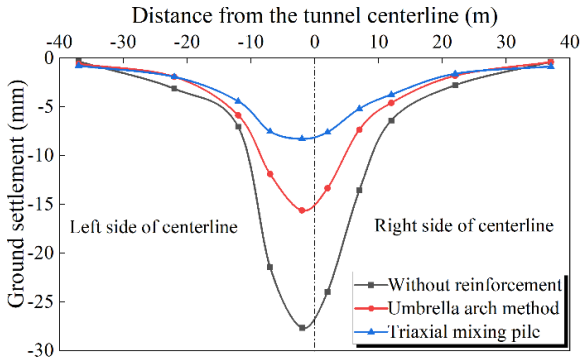

Fig. 4 Ground settlement curve of transverse section under distinct reinforcement approaches

Fig. 4 illuminates the ground settlement at the same transverse section of the shield upon arrival, obtained through simulation using different reinforcement approaches. The settlement curve is asymmetric and approximately V-shaped. The maximum settlement deviates from the tunnel centerline towards the direction of the left side which is already subjected to excavation. The surrounding soil at the left is reinforced by synchronous grouting after tunneling, which results in a better performance in overall strength and stability.

The results illustrated in Fig. 4 indicate a significant reduction in ground settlement after reinforcement. Specifically, the maximum ground settlement decreased from 27.7 mm with no reinforcement to 15.6 mm after adopting UA, and to 8.9 mm after TMP treatment. The TMP performs better than UA in terms of reducing ground settlement. This is attributed to the TMP is implemented through mixing the slurry with in-situ soil by stirring, resulting in less disturbance to the surrounding soil compared with UA. Additionally, the reinforcement zone of TMP is larger than that of UA. Notably, the reinforcement mechanism of UA relies on two parts, namely the grouted steel pipes erected ahead of the tunnel face and the injected cement grouting, both of which do not involve any construction on ground surface. Therefore, UA is only preferable when reinforcement from the ground surface is not optional.

4. Parametric study

Previous section has validated that TMP is a preferrable pre-reinforcement method against UA in cases when construction on ground surface is allowable. To further reduce ground settlement more effectively, it is necessary to quantitatively determine the optimal system parameters.

4.1 Reinforcement zone

The determination of reinforcement zone on ground settlement was divided into two steps: (1) The reinforcement depth was fixed at 0.5D (where D is the tunnel diameter) above the tunnel vault to 0.5D below the tunnel arch bottom, with the pile length ratio (short pile: long pile) and tunnel buried depth of 1:2 and 3.0D,

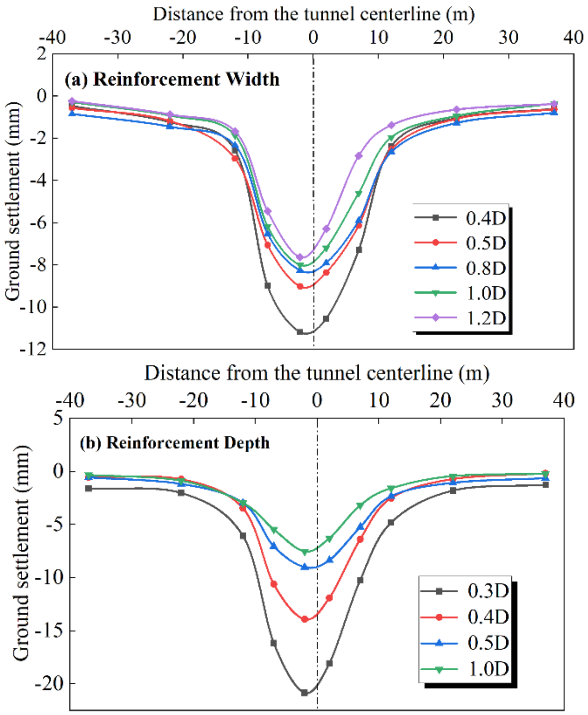

Fig. 5 Curve diagram of ground settlement varying with reinforcement range of short pile

respectively. The reinforcement width was then adjusted to be 0.4, 0.5, 0.8, 1.0, and 1.2D on both sides of the tunnel; (2) The reinforcement width, pile length ratio, and tunnel buried depth were fixed at 0.5D, 1:2, and 3.0D, respectively. The reinforcement depth was then selected as 0.3, 0.4, 0.5, and 1D.

Fig. 5 presents the variation of the ground settlement curves with different sizes of the reinforcement zone. The shapes of the ground settlement curves are similar with a slight variation in the maximum ground settlement. This variation mainly occurred near the centerline of the tunnel, and the settlement gradually decreased with increasing distance from the tunnel centerline. Moreover, there exist a critical reinforcement range for the impact on ground settlement. As depicted in Fig. 5(a), an increase in the reinforcement width from 0.4D to 1.2D resulted in a sharp decline in the maximum ground settlement from 11.2 mm (0.4D) to 9.0 mm (0.5D), followed by a continuous decrease to 7.5 mm (1.2D). This phenomenon is attributed to the fact that the soil disturbance caused by excavation decreases as the distance from the tunnel increases. Therefore, to effectively control ground settlement, it is recommended to use a reinforcement width of 0.5D, which strikes a balance between reinforcement effectiveness and cost-effectiveness.

As shown in Fig. 5(b), the resistance of the reinforced body was insufficient to effectively restrain soil deformation when the reinforcement depth was 0.3D, resulting in a maximum ground settlement exceeding 20 mm. However, the ground settlement was reduced to 9.0 mm when the reinforcement depth was increased to 0.5D, which was only 32.5% of the settlement without reinforcement. Further increasing the reinforcement depth

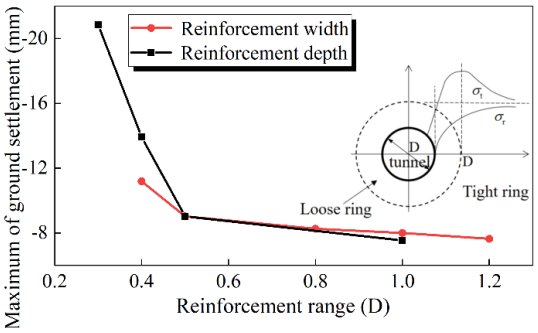

Fig. 6 Maximum of ground settlement under different reinforcement ranges

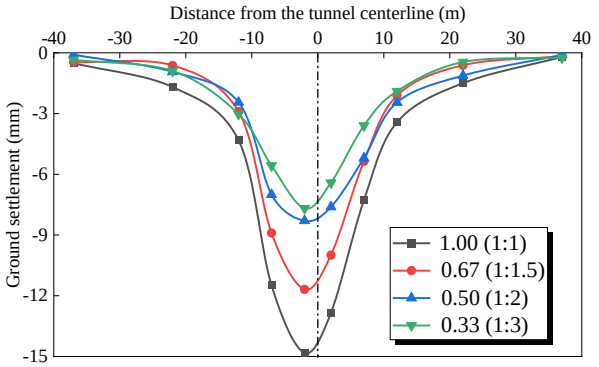

Fig. 7 Ground settlement curve of transverse section under different pile length ratio

to 1D only slightly reduced the ground settlement due to the limited range of soil disturbance during tunneling. Therefore, the optimal reinforcement depth is recommended to be from 0.5D above the tunnel vault to 0.5D below the tunnel arch bottom.

Fig. 6 depicts the maximum ground settlement with different sizes of reinforcement zones. The results indicated that the influence of the depth on ground settlement was greater than that of the width within a reinforcement of 0.5D. This is because the stratum loss mainly concentrates above the tunnel. The impact on settlement caused by the reinforcement range beyond 0.5D is almost the same. In addition, the disturbed soil resulted in localized stress variation, which means that there exists an optimal reinforcement range. As shown in Fig. 6, the soil redistributes from the three-dimensional stress state to the radial stress σ_r and tangential stress σ_t, forming two regions around the tunnel, i.e., the loose ring (stress-concentrated area), and the tight ring (stress-relaxed area). The stress in the tight ring is unable to transfer effectively to the distant soil. Therefore, timely and effective reinforcement can limit soil deformation and reduce the expansion radius of the plastic zone. In this case, the range of 0.5D outside the tunnel has already offset most of the stress and deformation.

Sufficient self-stiffness and total stability of the cement-soil mixture is the key to ensure minimal settlement, where pile stability is achieved by inserting the pile into the firm layer generally. However, in areas where the soft stratum is particularly thick, this will result in high cost of the project. To achieve both effectiveness and economy, this study adopts a long and short pile arrangement, where the depth of the long pile is determined by the ratio of long and short piles. The results of ground settlement under different pile length ratios are presented in Fig. 7. It can be observed that with an increase in the pile length ratio, the settlement decreases. This is attributed to the increased friction caused by the increased contact surface between the pile and the surrounding soil, which in turn improves the integrity of the cement-soil mixture. The maximum ground settlement was 14.8 mm when the pile length ratio was 1:1, while it was significantly reduced to 6.4 mm (43.2%) with a pile length ratio of 1:2. As the pile length ratio increased from 1:2 to 1:3, the reduction in settlement was only 1.3 mm (7.7%). Therefore, it can be concluded that the optimal reinforcement effect can be achieved when the pile length ratio is 1:2.

4.2 Tunnel buried depth

Considering the complexity of the ground conditions in the study area, it is necessary to conduct a thorough analysis of the buried depth of tunnels to determine the most feasible alternative. In this study, a parameter based on varying tunnel buried depths was used for modeling, and the buried depths considered were set at 1.5D (9 m), 2D (12 m), 2.5D (15 m), 3D (18 m), and 3.5D (21 m). The influence of varying tunnel buried depths on ground settlement is presented in Fig. 8. The results indicate that with increasing buried depth, the ground settlement gradually decreases between the inflection point on both sides of the centerline, while the opposite trend is observed outside the inflection point on both sides. Furthermore, as the ground settlement increases, the width of the settlement trough becomes narrower, which is attributed to the soil near the centerline of the tunnel sinking and exerting a squeezing effect on the soil on both sides and the effect becomes more pronounced with the increase of the settlement. Moreover, after a certain buried depth (3D), the influence on the vertical displacement stabilizes. Therefore, it is recommended to control the buried depth of the tunnel around 3D, which can effectively reduce ground settlement. Additionally, Fig. 9 depicts the impact of different tunnel buried depths on ground settlement. The settlement trough curve is relatively deep and narrow at a shallow buried depth of the tunnel since the range of soil disturbance is limited. The ground settlement trough gradually changes from an approximate V-type to W-type, which indicates that under shallow buried depth, the superposition effect between double-track tunnels is smaller.

Based on a large number of measured data, Zhu (2021) concluded that the settlement trough shape is approximately a primary function of H/D and L/D. Fig. 9 shows the dividing curve of the settlement curve form. When the location parameter coordinates of the tunnel are in the lower region of the function, the ground settlement trough form is single-peaked (i.e., V-type). On the other hand, when the location parameter coordinates are in the upper region of the function, the settlement trough form is double-peaked (i.e., W-type). In this study, L/D = 1.5, which corresponds to the curve H/D = 2.15, indicating that the settlement curve is double-peaked W-shaped when H/D is less than 2.15 and

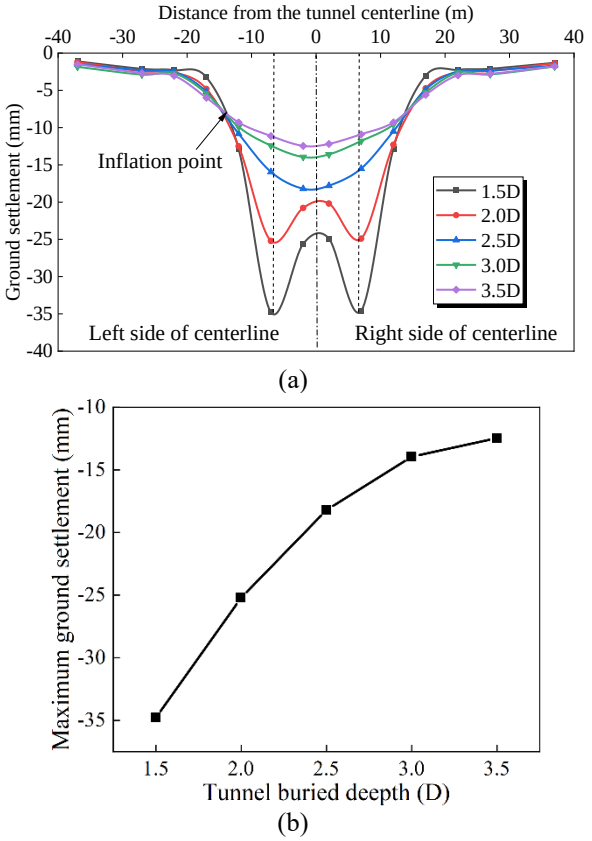

Fig. 8 Ground settlement curve of transverse section under tunnel buried depth

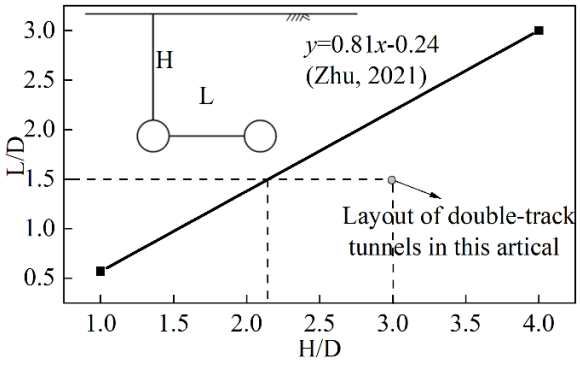

Fig. 9 Settlement trough shape boundary curve

single-peaked V-shaped when it is greater than 2.15. This is consistent with the change of curve shape observed in this study, suggesting that the tunnel spacing and burial depth primarily influence the settlement trough shape, while the influence of the stratum is smaller.

4.3 Pressure of tunnel face

The excavation process of a slurry shield involves resisting earth pressure and water pressure by utilizing the hydraulic pressure of the muddy water. The pressure generated is commonly referred to as the tunnel face pressure and its value is highly dependent on the soil constraint conditions (Park 2022). Determining a suitable range for the face pressure is of utmost importance to

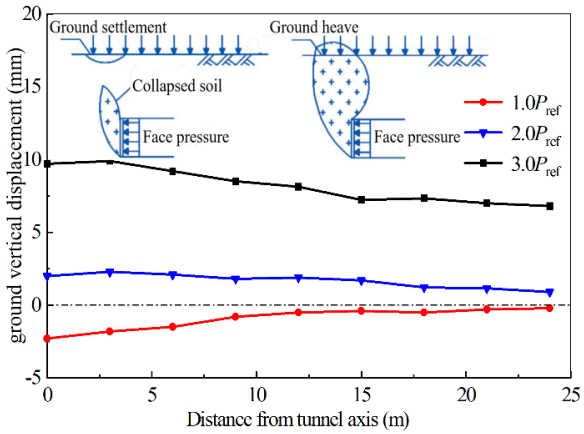

Fig. 10 Vertical displacement curve of transverse section under Tunnel face pressure

ensure the safety and cost-effectiveness of the tunnel construction. Generally, the face pressure is set to exceed the static earth pressure P_0, which can be calculated using the following formula

$$P_0 = (1-\sin\theta_i)\cdot\gamma_i\cdot h_i \quad (1)$$

Where θ_i is friction angle (°), γ_i denotes bulk weight of overburden soil (kN·m^{-3}) , h_i is thickness of stratum (m). When adopting the cement-soil mixing method to reinforce soft foundation, the bulk weight of slurry mixed into the soft soil is similar to that of in-situ soil. Therefore, the bulk weight of the cement-soil mixture is approximately taken as the bulk weight of natural soil, and the friction angle of the cement-soil mixture is taken as 45° for safety. Without considering groundwater, the static soil pressure P_0 at the tunnel face pressure can be calculated using formula (1) as P_0 = 170 KPa. Taking P_{ref} = 0.17 MPa as the reference equilibrium pressure, the analysis was conducted for three values of the pressure of tunnel face, namely P_{ref}, $2P_{ref}$, and $3P_{ref}$.

Fig. 10 illustrates the vertical displacement curve of the transverse section under varying tunnel face pressure. The magnitude of ground displacement increased as the distance from the central axis of the tunnel decreased, with the displacement peak value observed on the central axis. Furthermore, as the pressure increased, the deformation changed from settlement to heave. Settlement occurred when the tunnel face pressure (P_{ref}) was smaller than the lateral earth pressure, leading to the squeezing of the surrounding soil towards the inner side of the cutter head. Conversely, when the pressure ($2P_{ref}$) exceeded the lateral earth pressure, the deformation presented a heave. Beyond the pressure of $2P_{ref}$, the ground deformation in front of the cutter head gradually increased. However, the vertical displacement difference was slight when the tunnel face pressure varied between P_{ref} ~ $2P_{ref}$, indicating that the stratum after reinforcement withstands a wider range of variation of tunnel face pressure. Additionally, the preferred face pressure results are consistent with the (1.4~1.6) P_0 provided by Mao (2006), suggesting that reinforcement has little effect on the tunnel face pressure and is mainly

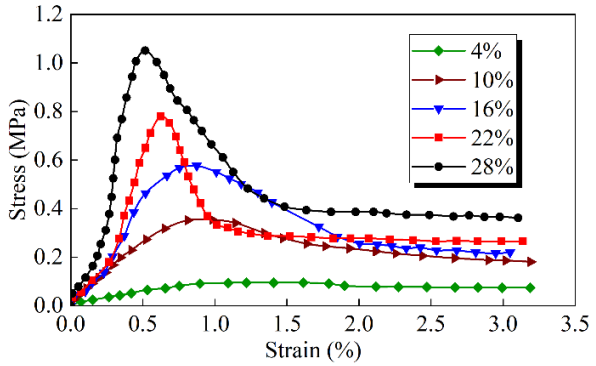

Fig. 11 Stress-strain relationship under different cement ratios

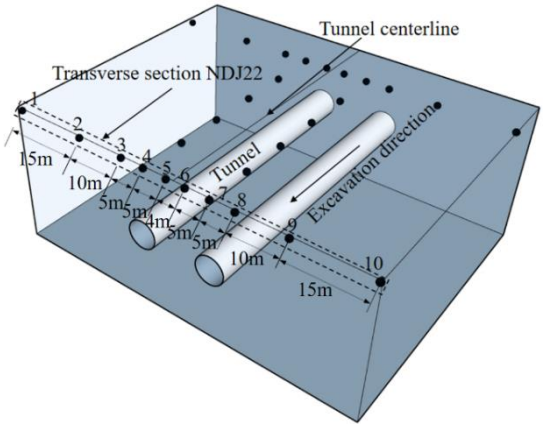

Fig. 12 Diagrammatic drawing of monitoring point layout

influenced by the tunnel buried depth and geological properties. Based on the most unfavorable working conditions and safety factors, the range of tunnel face pressure between $P_{ref} \sim 2P_{ref}$ was recommended as it was rational for resisting earth pressure.

5. Engineering application

5.1 Project reinforcement scheme

According to the research results of numerical simulation and combined with the actual situation, the grid type TMP was finally utilized for pre-reinforcement in this project, using parameters optimized in the previous numerical simulation (the range of short pile and the buried depth of the tunnel were set to be 0.5D and 3D, respectively, the depth of long pile is set to 2 times of short pile, and the face pressure was to be within $P_{ref} \sim 2P_{ref}$).

To determine the project configuration of slurry through the mechanical properties of the cement-soil mixture, this section investigated the stress-strain relationship curves of mucky silty clay at diverse cement incorporation ratios (4%, 10%, 16%, 22%, 28%) at a 28-day curing period. As shown in Fig. 11, with the increase of cement admixture ratio, the compressive strength of soil sample gradually increases and the brittle characteristic gradually became obvious, this was since the brittle characteristics of the cement-soil mixture were obvious when the cement admixture reached a certain amount, which was typical of brittle damage. Besides, the maximum stress appeared at a smaller strain (before 1%) after the cement incorporation ratio reached 22%, and the peak shear strain increased gradually with decreasing incorporation ratio, while the stress grown slowly with increasing strain at low cement incorporation ratio. Combined with the specific working conditions of the project, it is recommended that the compressive strength of the mixture design should be maintained at a minimum of 0.8 MPa. Accordingly, it is deemed appropriate to select a cement admixture ratio of 22%.

The interval reinforcement adopted φ850@600 triaxial mixing pile (i.e., the effective cross-sectional area of the single pile was 1.495 m^2), the amount of P.O 42.5 silicate cement in the slurry, average unit weight of stratum and the water-cement ratio in the field were 22%, 1.8×10^3 kg /m^3 and 1.5~2.0, respectively, then the amount of cement per meter for a single pile was 1800 kg/m^3×1.495 m^2×1 m×22 %=592 kg, and the amount of cement slurry per meter for a single pile was 592 kg + 592 kg× (1.5~2.0) = (1.48~1.78)× 10^3 kg.

To monitor the ground settlement, 10 measuring points were installed transversely every 50 m in the tunnel, and symmetrically arranged from the centerline of the tunnel to the two sides at a distance of 2 m, 7 m, 12 m, 22 m and 37 m respectively, the specific arrangement of the monitoring point is depicted in Fig. 12.

5.2 Discussion of settlement and modified model

In this section, some research methods and results on ground settlement are discussed, and modified based on existing models, a modified model is developed to simplify the prediction of the ground settlement trough curve of the reinforced stratum.

The concept of settlement trough curve conforming to Gaussian distribution was first proposed by Peck (1969), who also developed an empirical model for predicting ground settlement.

$$S(x) = \frac{V_l}{\sqrt{2\pi} \times i} \exp(-\frac{x^2}{2i^2}) \quad (2)$$

Where x is the distance from tunnel centerline (m), $S(x)$ is the ground settlement value at x from the tunnel centerline (mm), i is settlement trough width (m) and V_l is stratum loss per unit length of tunnel. Subsequently, various studies revolve around the modification of parameters i and V_l in the Peck model to suit different construction condition. In this study, the stratum loss rate is based on the experience of the Foshan soft soil area (Wu and Zhu 2018), and the average value is V_l = 1.57%. Settlement trough width i is determined through an empirical method developed by Mair *et al.* (1993), i.e., Eq. (3).

$$i = K(H - z) \quad (3)$$

Where K is a constant for a specific depth, z is depth of the settlement trough from the ground surface (m). Wang *et*

al. (2016) obtained (H - z) / H = -2.8 K + 2.1 through extensive model tests. When z takes the value of 0, K=0.4, and then Eq. (4) is obtained as ground settlement model.

$$S(x)=\frac{V_l}{\sqrt{2\pi}\times KH}\exp[-\frac{x^2}{2(KH)^2}]=2.63\exp(-\frac{x^2}{2\times 7.2^2}) \quad (4)$$

However, numerous studies have taken inconsistent estimates of parameter i. Therefore, considering the non-uniform stratum loss during shield tunneling, Sagaseta (1987) proposed an equivalent ground loss model without parameter i

$$S(x)=\frac{V_l}{\pi}\cdot\frac{H}{x^2+H^2} \quad (5)$$

Where, H is the buried depth of tunnel (m). Based on a large number of measurement data of tunnel excavation. However, none of the above models have specific application specific soil layers. Therefore, Loganathan and Poulos (1998) proposed a non-uniform radial analytic solution suitable for clays (6)

$$S(x)=S_{\max}\cdot\exp\left[\frac{-1.38x^2}{(H+D/2)^2}\right] \quad (6)$$

Where $S_{\max}$ is the maximum of ground settlement (mm). Regarding complex conditions with limited data, $S_{\max}$ is difficult to obtain in the Loganathan model, Therefore, the Sagatega solution is used to estimate this value.

$$S_{\max}=\frac{V_l}{\pi H} \quad (7)$$

In order to optimize the calculation, this paper assumes that the settlement trough of the double track tunnel remains axisymmetric, hence the obtained model results are all shifted to the left by 2 m. As depicted in Fig. 14, the results of the above models do not agree with the measured results, it is attributed to that these models have great regional limitations and none of them consider the effect of pre-reinforcement on ground settlement. Therefore, considering that the soil disturbance decreases exponentially with increasing off-axis distance (Zhou *et al*. 2021), this paper introduces the disturbance correction coefficient $\xi(x)$ to predict ground settlement.

$$\xi(x)=C+C(e^{-0.004x^2}-1) \quad (8)$$

Where C is coefficient related to the layout of two tunnels, operating condition (Shield tail clearance, turning radius of the tunnel, and grouting effect), and geological condition. the maximum $\xi(x)$ is C above the axis, and the minimum $\xi(x)$ is close to 0 at the edge of the settlement trough. Modified based on existing models，the new model is as follows

$$S(x)=\frac{\xi(x)\cdot V_l}{\pi H}\cdot\exp\left[\frac{-1.38x^2}{(H+D/2)^2}\right] \quad (9)$$

When C = 0.321 is basically the same as the measured settlement curve, hence the ground settlement caused by tunneling after pre-reinforcement can be modified as

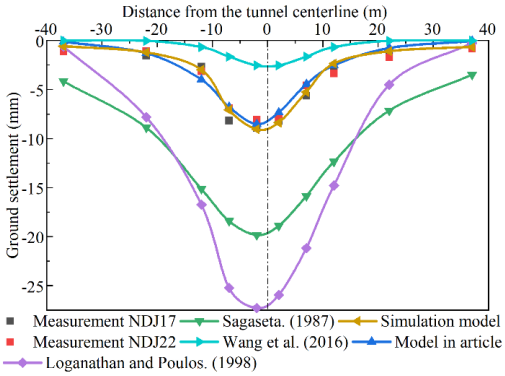

Fig. 13 Measurement and diverse models results of ground settlement

$$S(x)=\frac{\left[0.321+0.321(e^{-0.004x^2}-1)\right]\cdot V_l}{\pi H}\cdot\exp\left[\frac{-1.38x^2}{(H+D/2)^2}\right] \quad (10)$$

Fig. 13 displays a comparison between the measured settlement data and the results obtained from various models. The settlement predictions from Sagaseta (1987) and Loganathan and Poulos (1998) are obviously excessive, mainly because they neglect the impact of soft soil reinforcement on reducing ground settlement. On the other hand, Wang *et al*. (2016) underestimate the settlement value since they fail to consider the superposition effect of the double line on the settlement. In contrast, the simulation and modified model proposed in this article demonstrate good agreement with the measured data. These results rationally reflect the actual settlement on the site and highlight the superiority of the modified model compared to existing models.

6. Conclusions

Numerical simulation was adopted to evaluate the performance of TMP and UA for ground settlement control and determine the optimal system parameters for the implementation of TMP during shield tunneling in soft stratum, and the preferable method (i.e. TMP) was applied to Chuangju shield section project of Foshan Metro Line 3. In addition, by taking advantage of field measurement data, a modified model was developed to predict the ground settlement of similar pre-reinforcement projects. The following conclusions can be drawn:

- The ground settlement is primarily caused by soil deformation at the gap between the shield and segment and can be significantly reduced by pre-reinforcement. Compared to the scenario without reinforcement, the ground settlement can be reduced by 43.7% using the UA, 67.5% using the TMP with optimal system parameters.
- TMP outperforms UA in settlement reduction and applicability, making it the preferred option for long-distance pre-reinforcement projects. There exists a critical reinforcement range (approximately 0.5D in this study) when the TMP was adopted for reinforcement, within which

the ground settlement decreases rapidly with the increase of the reinforcement range, and sensitivity of ground settlement to the reinforcement depth was greater than that to the reinforcement width; however, beyond the critical value, the reinforcement range only demonstrate a slight impact and difference on reducing ground settlement. For better reinforcement benefits, it was recommended that the reinforcement depth of short piles should be controlled from 0.5D above the tunnel vault to 0.5D below the tunnel arch bottom, the length of long piles should be controlled at twice the length of short piles, and the reinforcement width should be 0.5D on both sides of the tunnel.

• The shape of ground settlement trough changes from approximate W-type to V-type with the increase of buried depth. There are two inflection points, and the maximum ground settlement between the inflection points gradually decreases and tends to be stable after 3D. Meanwhile, it gradually increases outside the inflection points. The deformation of the soil in front of the cutter head changes from settlement to heave with the increase of the face pressure when the buried depth of the tunnel is 3D. Besides, the stratum after reinforcement withstands a wider range of variation of tunnel face pressure, and it is relatively balanced with the surrounding earth pressure under the face pressure of $P_{ref} \sim 2P_{ref}$, with little disturbance to the soil.

• The disturbance correction coefficient $\xi(x)$ is introduced to correct stratum loss rate, and it varies exponentially with distance x from the axis of the tunnel. The results of simulation and the modified model in this article for ground settlement are in good agreement with the measurement results, and equivalent ground loss models based on soft ground are better applied to modify and predict ground settlement for double track tunnel after pre-reinforcement.

Acknowledgments

The authors would like to acknowledge the financial support provided by the National Natural Science Foundation of China (No. 031050050).

References

An, J.B., Kang, S.J., Kim, J. and Cho, G.C. (2022), "Numerical evaluation of surface settlement induced by ground loss from the face and annular gap of EPB shield tunneling", *Geomech. Eng.*, **29**(3), 291-300. https://doi.org/10.12989/gae.2022.29.3.291.

Benz, T. (2007), "Small-strain stiffness of soils and its numerical consequences (Vol. 5)", Stuttgart: Univ. Stuttgart, Inst. f. Geotechnik.

Chakeri, H., Hasanpour, R., Hindistan, M.A. and Ünver, B. (2011), Analysis of interaction between tunnels in soft ground by 3d numerical modeling", *Bull. Eng. Geol. Environ.*, **70**(3), 439-448. https://doi.org/10.1007/s10064-010-0333-8.

Consoli, N.C., Faro, V.P., Schnaid, F. and Born, R.B. (2017), "Stabilised soil layers enhancing performance of transverse-loaded flexible piles on lightly bonded residual soils", *Soils Rocks*, **40**(3), 219-228. https://doi.org/10.28927/sr.403219.

Deng, H.S., Fu, H.L., Yue, S., Huang, Z. and Zhao, Y.Y. (2022), "Ground loss model for analyzing shield tunneling-induced surface settlement along curve sections", *Tunn. Undergr. Sp. Tech.*, **119**: 104250. https://doi.org/10.1016/j.tust.2021.104250.

González, L., Abdoun, T. and Dobry, R. (2009), "Effect of soil permeability on centrifuge modeling of pile response to lateral spreading", *J. Geotech. Geoenviron. Eng.*, **135**(1), 62-73. https://doi.org/10.1061/(ASCE)1090-0241(2009)135:1(62).

Kasper, T. and Meschke, G. (2006), "On the influence of face pressure, grouting pressure and TBM design in soft ground tunnelling", *Tunn. Undergr. Sp. Tech.*, **21**(2), 160-171. https://doi.org/10.1016/j.tust.2005.06.006.

Liang, R.Z., Xia, T.D., Lin, C.G. and Yu, F. (2015), "Analysis of ground surface displacement and horizontal movement of deep soils induced by shield advancing", *Chinese J. Rock Mech. Eng.*, **34**(3), 583-593. https://doi.org/10.13722/j.cnki.jrme.2015.03.016.

Liang, Y., Chen, X., Yang, J., Zhang, J. and Huang, L. (2020), "Analysis of ground collapse caused by shield tunnelling and the evaluation of the reinforcement effect on a sand stratum", *Eng. Fail. Anal.*, **115**, 104616. https://doi.org/10.1016/j.engfailanal.2020.104616.

Lv, C.Y., Guo, Y.C., Li, Y.H. and Yao, W.M. (2023), "Experimental study on the horizontal bearing characteristics of long-short-pile composite foundation", *Geomech. Eng.*, **33**(4), 341-352. https://doi.org/10.12989/gae.2023.33.4.341.

Lv, J., Li, X., Li, Z. and Fu, H. (2020), "Numerical smulations of construction of shield tunnel with small clearance to adjacent tunnel without and with isolation pile reinforcement", *KSCE J. Civil Eng.*, **24**, 295–309. https://doi.org/10.1007/s12205-020-1167-y.

Liu, S.Y., Du, Y.J., Yi, Y.L. and Puppala, A.J. (2012), "Field investigations on performance of T-shaped deep mixed soil cement column–supported embankments over soft ground", *J. Geotech. Geoenviron. Eng.*, **138**(6), 718-727. https://doi.org/10.1061/(ASCE)GT.1943-5606.0000625.

Loganathan, N. and Poulos, H.G. (1998), "Analytical prediction for tunneling induced ground movements in clays", *J. Geotech. Geoenviron. Eng.*, **124**(9), 846-856. https://doi.org/10.1061/(ASCE)1090-0241 (1998) 124:9(846).

Mu, B., Xie, X., Li, X., Li, J.C., Shao, C.M. and Zhao, J. (2021), "Monitoring, modelling and prediction of segmental lining deformation and ground settlement of an EPB tunnel in different soils", *Tunn. Undergr. Sp. Technol.*, **113**, 103870. https://doi.org/10.1016/j.tust.2021.103870.

Moon, J., Yoon, I., Kim, M., Lee, J. and Kim, Y. (2023), "Ultrasonically enhancing flowability of cement grout for reinforcing rock joint in deep underground", *Geomech. Eng.*, **33**(2), 211-219. https://doi.org/10.12989/gae.2023.33.2.211.

Morovatdar, A., Palassi, M. and Ashtiani, R.S. (2020), "Effect of pipe characteristics in umbrella arch method on controlling tunneling-induced settlements in soft grounds", *J. Rock Mech. Geotech. Eng.*, **12**(5), 984-1000. https://doi.org/10.1016/j.jrmge.2020.05.001.

Mair, R.J., Taylor, R.N. and Bracegirdle, A. (1993), "Subsurface settlement profiles above tunnels in clays", *Géotechnique*, **43**(2), 315-320. https://doi.org/ 10.1680/geot.1993.43.2.315.

Mao, C.J. (2006), "An inquisition into calculation of earth pressure of tunnel face for the slurry shield", *Constr. Machinery Technol. Management*, (4),70-73.

O'Reilly, M. and New, B. (1982), "Settlement above tunnels in the United Kingdom - Their magnitude and prediction. In: Tunnelling 82", *Proceedings of the 3rd International Symposium*, Institution of Mining and Metallurgy, London, UK.

Peck, R.B. (1969), "Deep excavations and tunneling in soft ground", *Proceedings of the 7th International Conference on Soil Mechanics and Foundation Engineering*, Mexico City, Mexico.

Phutthananon, C., Jongpradist, P., Dias, D. and Jamsawang, P. (2021), "Numerical study of the deformation performance and

failure mechanisms of TDM pile-supported embankments", *Transport. Geotech.*, **30**, 100623. https://doi.org/10.1016/j.trgeo.2021.100623.

Pan, H., Tong, L., Wang, Z. and Yang, T. (2022), "Effects of Soil–Cement Mixing Wall Construction on Adjacent Shield Tunnel Linings in Soft Soil", *Arabian J. Sci. Eng*., 1-15. https://doi.org/10.1007/s13369-022-06705-9.

Pei, X.J., Zhang, F.Y., Wu, W.J. and Zhang, S.Y. (2015), "Physicochemical and index properties of loess stabilized with lime and fly ash piles", *Appl. Clay Sci.*, **114**, 77-84. https://doi.org/10.1016/j.clay.2015.05.007.

Phutthananon, C., Jongpradist, P. and Jamsawang, P. (2020), "Influence of cap size and strength on settlements of TDM-piled embankments over soft ground", *Mar. Georesour. Geotec.*, **38**(6), 686-705. https://doi.org/10.1080/1064119X.2019.1613700.

Park, J.K. (2022), "Reliability analysis of tunnel face stability considering seepage effects and strength conditions", *Geomech. Eng.*, **29**(3), 331-338. https://doi.org/10.12989/gae.2022.29.3.331.

Qian, W., Qi, T., Zhao, Y., Le, Y. and Yi, H. (2019), "Deformation characteristics and safety assessment of a high-speed railway induced by undercutting metro tunnel excavation", *J. Rock Mech. Geotech. Eng.*, **11**(1), 88-98. https://doi.org/10.1016/j.jrmge.2018.04.014.

Qi, W., Yang, Z., Jiang, Y., Yang, X., Shao, X. and An, H. (2022), "Experimental study on fresh state properties of single-liquid semi-inert synchronous grouting for shield tunnels in water-rich sand strata", *Arabian J. Sci. Eng.*, **47**(4), 4639-4655. https://doi.org/10.1007/s13369-021-06220-3.

Rankin, W.J. (1988), "Ground movements resulting from urban tunnelling: Predictions and effects", *Geol. Soc.*, **5**(1), 79-92. https://doi.org/ 10.1144/ gsl.eng.1988.005.01.06.

Sagaseta, C. (1987), "Analysis of undrained soil deformation due to ground loss", *Geotechnique*, **37**(3), 301-320. https://doi.org/10.1680/geot.1987.37.3.301.

Song, Z., Tian, X. and Zhang, Y. (2019), "A new modified Peck formula for predicting the surface settlement based on stochastic medium theory", *Adv. Civil Eng.*, 2019, 1-14. https://doi.org/10.1155/2019/7328190.

Shao, X., Yang, Z., Jiang, Y., Yang, X. and Qi, W. (2022), "Field test and numerical study of the effect of shield tail-grouting parameters on surface settlement", *Geomech. Eng.*, **29**(5), 509-522. https://doi.org/10.12989/gae.2022.29.5.509.

Shu, B., Gong, H. and Chen, S. (2022), "Case study of solid waste based soft soil solidifying materials applied in deep mixing pile", *Buildings*, **12**(8), 1193. https://doi.org/10.3390/buildings12081193.

Schiena, F., Lusini, E., Fazio, A.L. and Graziani, A. (2024), "A strain applied method for FEM-2D modelling of TBM tunnels in coarse-grained soils with comparative analysis of case histories", *Tunn. Undergr. Sp. Tech.*, **153**, 106001. https://doi.org/10.1016/j.tust.2024.106001.

Verruijt, A. and Booker, J.R. (1996), "Surface settlements due to deformation of a tunnel in an elastic half plane", *Geotechnique*, **46**(4), 753-756. https://doi.org/10.1680/geot.1996.46.4.753.

Voottipruex, P., Bergado, D.T., Suksawat, T., Jamsawang, P. and Cheang, W. (2011), "Behavior and simulation of deep cement mixing (DCM) and stiffened deep cement mixing (SDCM) piles under full scale loading", *Soils Found.*, **51**(2), 307-320. https://doi.org/10.3208/sandf.51.307.

Wang, Z., Zhang, K.W., Wei, G., Li, B., Li, Q. and Yao, W.J. (2018), "Field measurement analysis of the influence of double shield tunnel construction on reinforced bridge", *Tunn. Undergr. Sp. Tech.*, **81**, 252-264. https://doi.org/10.1016/j.tust.2018.06.018.

Wang, F., Miao, L., Yang, X., Du, Y.J. and Liang, F.Y. (2016), "The volume of settlement trough change with depth caused by tunneling in sands", *KSCE J. Civil Eng.*, **20**(7), 1-6. https://doi.org/ 10.1007/s12205-016-0250-x.

Wu, C.S. and Zhu, Z.D. (2018), "Comparative study on ground loss ratio due to shield tunnel with different diameters", *Chinese J. Geotech. Eng.,* **40**(12), 2257-2265. http://doi.org/10.11779/CJGE201812013.

Yapage, N.N.S., Liyanapathirana, D.S., Kelly, R.B., Poulos, H.G. and Leo, C.J. (2014), "Numerical modeling of an embankment over soft ground improved with deep cement mixed columns: case history", *J. Geotech. Geoenviron. Eng.*, **140**(11), 04014062. https://doi.org/10.1061/(ASCE)GT.1943-5606.0001165.

Yao, X., Liu, K., Huang, G., Wang, M. and Dong, X. (2021), "Mechanical properties and durability of deep soil–cement column reinforced by jute and PVA fiber", *J. Mater. Civil Eng.*, **33**(4), 04021021. https://doi.org/10.1061/(ASCE)MT.1943-5533.0003636.

Yi, Y., Liu, S. and Puppala, A.J. (2016), "Laboratory modelling of T-shaped soil–cement column for soft ground treatment under embankment", *Géotechnique*, **66**(1), 85-89. https://doi.org/10.1680/jgeot.15.P.019.

Yamashita, K., Wakai, S. and Hamada, J. (2013), "Large-scale piled raft with grid-form deep mixing walls on soft ground", *Proceedings of the of 18th ICSMGE*, 2637-2640.

Zhang, Z., Chen, J., Zhang, M. and Yang, X. (2022), "Modified Peck method of evaluating tunnelling-induced ground movements based on measured data", *Arabian J. Geosci.*, **15**(9), 862. https://doi.org/10.1007/s12517-022-10142-1.

Zhou, Z., Ding, H., Miao, L. and Gong, C. (2021), "Predictive model for the surface settlement caused by the excavation of twin tunnel", *Tunn. Undergr. Sp. Tech.*, **114**, 104014. https://doi.org/10.1016/j.tust.2021.104014.

Zheng, L., Chen, Z.Q., Liu, W., Zeng, Z. and Gu, D. (2020), "Numerical simulation and analysis of the pile underpinning technology used in shield tunnel crossings on bridge pile foundations", *Undergr. Sp.*, **6**(4), 396-408. https://doi.org/10.1016/j.undsp.2020.05.006.

Zhao, Y., Yang, J. and Zhang, Y. (2019), "Failure behavior of tunnel lining caused by concrete cracking: a case study", *J. Fail. Anal. Prevention*, **19**, 1158-1173. https://doi.org/10.1007/s11668-019-00718-7.

Zhao, J., Yang, P., Li, L., Feng, J. and Zhou, Z. (2023), "Impact of MJS treatment and artificial freezing on ground temperature variation: A case study", *Geomech. Eng.*, **32**(3), 293-305. https://doi.org/10.12989/gae.2023.32.3.293.

Zhao, Y.H., Yang, P., Zhang, Y.W. and Wang, N. (2021), "Study on MJS+horizontal freezing reinforcement and thawing temperature field in the overlapped area of the underpass station", *J. Forestry Eng.*, **6**(4), 159-166.

Zhao, L., Chen, Y., Chen, W., Wang, J. and Ren, C. (2023), "The performance of T-shaped deep mixed soil cement column-supported embankments on soft ground", *Constr. Build. Mater.*, **369**, 130578. https://doi.org/10.1016/j.conbuildmat.2023.130578.

Zhang, X.Y., Zhu, H.B., Jiao, Z.Z. and Cen, Z.H. (2022), "Lattice-shaped ground improvement by mixing soil and alkali-activated slag for liquefaction mitigation", *Case Studies Constr. Mater.*, **17**, e01445. https://doi.org/10.1016/j.cscm.2022.e01445.

Zhu, L. (2021). "Behavior analysis of ground settlement induced by the construction of parallel shield tunnels", *J. Water Resour. Architect. Eng.*, **19**(3), 208-213

CC